Structural and mechanical properties of glassy and glass ceramic products from tannery ash stabilization

S. Varitis[(a)], P. Kavouras[(b)], G. Kaimakamis[(a)], G. Vourlias[(a)], E. Pavlidou[(a)], Th. Karakostas[(a)], Ph. Komninou[(a)]

(a) School of Physics, Aristotle University of Thessaloniki

(b) Department of Materials Science and Engineering, School of Chemical Engineering, National Technical University, Athens, Greece

Abstract

The aim of this work is to investigate the microstructure and microhardness of glassy and glass-ceramic products synthesized through vitrfication and devitrification of chromium containing tannery ash with SiO_2, Na_2O and CaO glass forming oxides. Four different batch mixtures were studied with varying proportions of chromium ash and glass formers. Electron Microscopy study was performed that included Scanning Electron Microscopy with Energy Dispersive Spectroscopy (SEM-EDS) to study the morphology and composition of the products in the microscale. Transmission Electron Microscopy (TEM) and High Resolution TEM (HRTEM) observations were conducted to investigate structures up to the atomic scale and to correlate the structural properties with the stabilization process. Static micro-indentation was applied, using Knoop geometry, to determine the microhardness of the products while Vickers geometry was used to study crack propagation on their surfaces in order to test their potential use in various applications. Out of one, the initial vitrified products were amorphous with Eskolaite (Cr_2O_3) flakes dispersed inside the silicate matrix while the product with the lowest relative proportion of chromium ash was a homogenous glass. Furthermore, thermal treatment was conducted to the vitrified products and resulted to the separation of Devitrite, Combeite and Wollastonite crystalline phases from the silicate matrix depending on the initial batch composition of the glasses and the relative thermal treatment. The microhardness of the products was higher after thermal processing and it has been shown that the morphology of the separated crystal phases affected also the crack propagation.

Keywords: tannery sludge, electron microscopy, vitrification, glass ceramics, chromium stabilization, microindentation

Introduction

Tannery produces large amounts of chromium-containing sludge with high organic content [1] Disposal of this waste is one of the major problems in tannery industry while the effluents are ranked between the highest pollutants among all industrial wastes [2]. The main problems of tannery wastes are the containing chromium and the organic content. Despite the fact that tannery sludge contains trivalent chromium, which is thermodynamically stable, the presence of naturally occurring minerals which can act as oxidizing factors, such as Mn oxides in the environment, can enhance the oxidation of Cr^{3+} to Cr^{6+} in the soil [3].

Vitrification is a very advantageous and well established technology which makes possible the conversion of inorganic wastes into stable glasses. The main advantage is that it is possible to achieve chemical stabilized monolithic vitreous products via incorporation of toxic inorganic elements inside the vitreous matrix which could be safely landfilled. Additionally, it is important that except from stabilization, the volume of the wastes can be also significantly decreased [4]. Further thermal treatment of these products can result to potential marketable glass-ceramic products which can reduce the overall cost of vitrification [5].

Electron microscopy study of the stabilized products is important since it can provide information about the composition and the morphology of the vitreous matrix and the separated crystalline phases inside it due to the dispersion of various phases through the glass matrix. Moreover in combination with X-Ray Diffraction (XRD) analysis it provides a complete structural characterization of the final products. Utilization of electron microscopy techniques can result to complete study from the microscopic (SEM) to the nanoscopic (TEM) scale. On the other hand it is very important to study the micro-hardness and the crack propagation of stabilized vitreous and glass-ceramic products. First it can indicate how the products could retain their structural integrity after landfilling since they will be under pressure due to the above overload [6]. Moreover it would indicate whether they could be used as structural materials in various applications.

The current work aims to the investigation of vitrified and devitrified products resulting from vitrification of chromium containing tannery ash [7]. Utilization of conventional and high resolution TEM techniques, in addition to SEM and XRD, enabled the study of the structures up to the atomic scale and also the correlation of the nanostructure with the stabilization processing and the initial chemical composition. Moreover the separated crystalline phases before and after thermal treatment were verified. Knoop indentation tests were carried out in order to determine the microhardness of the resulting products while the study of the crack propagation was conducted using Vikers indentation.

Materials and Methods

Tannery waste was recovered from the industrial zone of Thessaloniki in northern Greece. This initial waste which had the form of a dry sludge was rich in trivalent chromium, calcium and had a very high organic content. This sludge was then treated thermally for 1,5h at 500°C under anoxic conditions (absence of oxygen) to remove the most possible organic content and to avoid oxidation of chromium in the hexavalent and dangerous form [7].

Vitrification was conducted using silica (SiO_2) as the main glass-former and soda ash (Na_2CO_3) and lime ($CaCO_3$), reagent grade, as network modifiers. All batch mixtures were melted in a Pt crucible at 1400°C or 1500°C, depending on the batch composition, for two hours in order to achieve a homogenous melt. Then the melt was casted in air on a refractory steel plate to as to cool rapidly. The resulting vitrified products were treated thermally at specific temperatures, determined by DTA analysis, so as to obtain the devitrified products. Duration of thermal treatment was 30 min, so as there would be enough time for the glass-formers and fluxes to diffuse and allow crystallization [8].

Structural characterization of the products was conducted using X-Ray diffraction (XRD) with a Rigaku powder diffractometer, using CuKa1 radiation. Morphology of the samples was examined using Scanning Electron Microscope (SEM) with a JEOL JSM-840A electron microscope so as with a Zeiss Axiolab-A metallographic microscope. Elemental analysis was conducted with Energy Dispersive Spectrometry (EDS) with an OXFORD ISIS-300 EDS analyzer, attached on the SEM instrument.

Samples for TEM-HRTEM observations were prepared in plan-view direction. Initial samples were cut in slices and mechanically grinded. Mechanical grinding was followed by low-voltage Ar^+ precision ion-milling (Gatan PIPS) to achieve electron transparency. Transmitting Electron Microscopy (TEM-HRTEM) observations were conducted using Jeol 2011 electron microscope operating at 200kV with a point resolution of 0.194nm and C_s=0.5mm. Elemental analysis with energy-dispersive X-ray spectroscopy (EDS), was performed using an Oxford Instruments INCAx-sight liquid nitrogen cooled detector with an ultrathin window attached on a Jeol 2011 electron microscope.

The microhardness of the vitrified and devitrified products was determined by static micoindentation with a Knoop indenter geometry using an Anton-Paar MHT-10 microhardness tester, attached on a Zeiss Axiolab-A optical microscope. Knoop indentations were conducted under load of 100g, contact time 10s and slope 20g/s using the following equation (1):

$$H_K = 12{,}229 * 9{,}81 \frac{P}{d^2} \text{ (GPa)}, \qquad (1)$$

where H_K is the Knoop hardness, P is the applied load and d is the length of the long diagonal imprint. In Vickers geometry higher load of 200g was applied to all samples in order to produce cracks on the surfaces.

Results and Discussion

Tannery ash

The waste used for the stabilization process had the form of a dry chromium containing ash. This ash is originated from the incineration of tannery sludge under anoxic conditions (absence of oxygen) at 500°C for 1,5h. The main crystal phases contained in the chromium ash were two $CaCO_3$ polymorphs, Calcite and Aragonite [7] while no Cr-containing crystalline phase was detected.

Vitrification products

Vitrification of tannery ash was conducted using additional glass froming (SiO_2) and network modifying (Na_2O and CaO) oxides since chromium ash (Cr-ash) had high CaO content but very low content of the other glass forming oxides and network modifiers. Four different batch compositions were studied with varying proportions of glass formers, network modifiers and Cr-ash. SiO_2 was about 55-56 wt%, Na_2O and CaO (table 1) varied in order to keep the liquidus as low as possible since Cr has low solubility in the silicate melts [9]. Variation of Cr-ash was between 10wt% and 20wt%.

Table 1: The % wt. proportions of Cr-ash and vitrifying agents in the six different batches.

Product	Ash	SiO_2	Na_2O	CaO	Si/O
P1	20	55	15	10	0.37
P2	15	55	15	15	0.37
P3	13	56	5	26	0.36
P4	10	55	15	20	0.36

After casting, the vitrified products looked homogenous in optical inspection and had a dark green to black color. XRD analysis indicated that except from P4, vitrified products were amorphous with Cr_2O_3 peaks superimposed on the amorphous background (Fig. 1). P4 was totally amorphous without any indication of separated crystalline peaks on the amorphous curve.

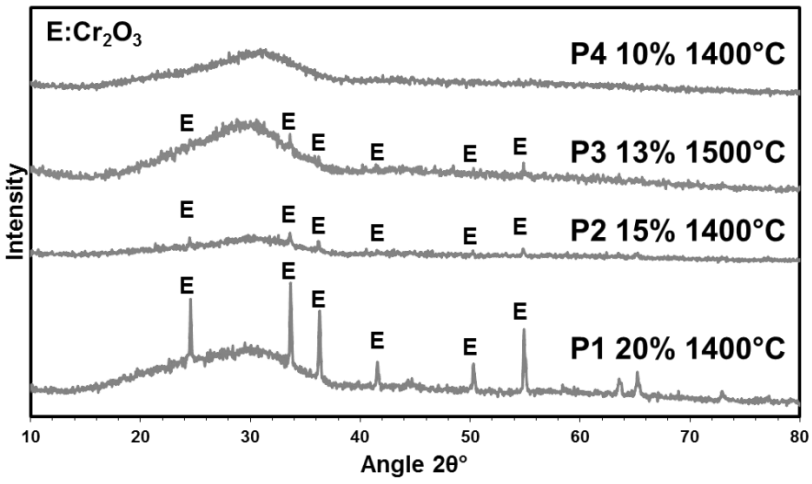

Figure 1: XRD graph of the as-vitrified products

SEM and TEM study shown that there were separated flake-like crystallites embedded in the silicate matrix for the most of the cases. EDS analysis on these dispersed crystallites verified that they were mainly composed of chromium. In comparison to the XRD results it was concluded that these crystallites are Eskolaite (Cr_2O_3) crystallites. EDS study on the amorphous matrix showed that the glass-forming elements were homogenously dispersed and Cr was incorporated in the matrix in different proportions depending on the initial batch composition and they are listed in Table 2.

Table 2 Atomic percentage of chromium in the glass matrix and total Cr content in the as-vitrified products measured by SEM-EDS.

Product	Cr matrix (at%)	Total Cr content (at%)
P1	1.6 ±0.3	4.5 ±0.4
P2	2.2 ±0.3	3.3 ±0.3
P3	2.1 ±0.2	3.3 ±0.9
P4	2.4 ±0.6	2.4±0.6

Chromium content inside the silicate matrix varied between 1.6 at% (P1) up to 2.4 at% (P4). It seems that as the Cr-ash loading increases the amount of incorporated Cr in the matrix is decreasing and the remaining is separated in the form of Cr_2O_3 crystallites. As it is reported from D. Huang et. al (2004) [10] when Cr reaches the solubility limit the exceeded Cr is separated in a chromium containing crystal phase.

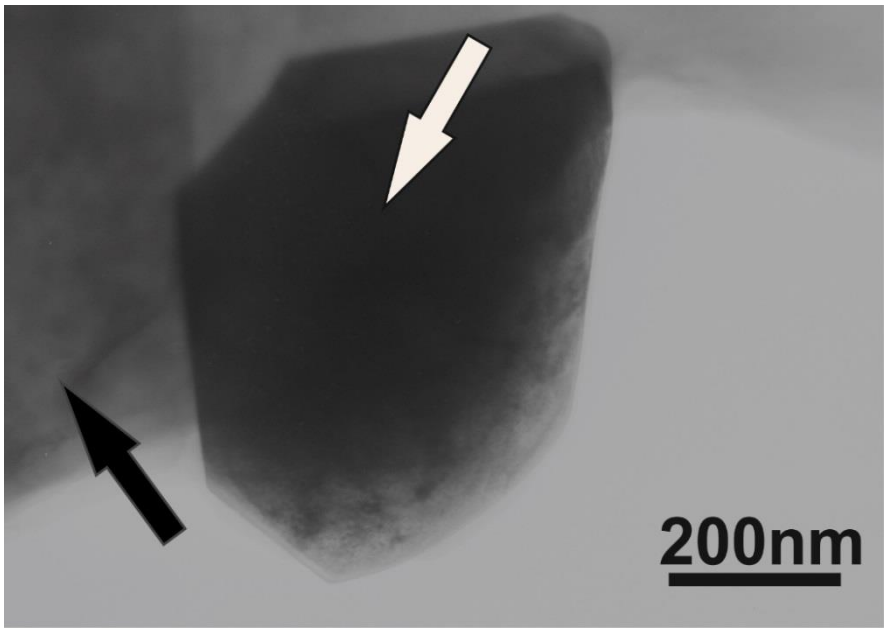

Figure 2. TEM image from the as-vitrified product P1 depicting a separated Eskolaite crystallite. The white arrow indicates the Cr_2O_3 crystallite and the black arrow the amorphous matrix.

The crystal structure of Eskolaite was studied combining the HRTEM observations and the Electron Diffraction Pattern (EDP) as it is depicted in **Figures 2** and **3**. Both the HRTEM image and the diffraction pattern are recorded along the [$\underline{2}$ $\underline{4}$ $\underline{1}$] zone axis. The above analysis showed that these crystallites correspond to Eskolaite (Cr_2O_3) (PDF# 38-1479) with hexagonal structure (R-3c).

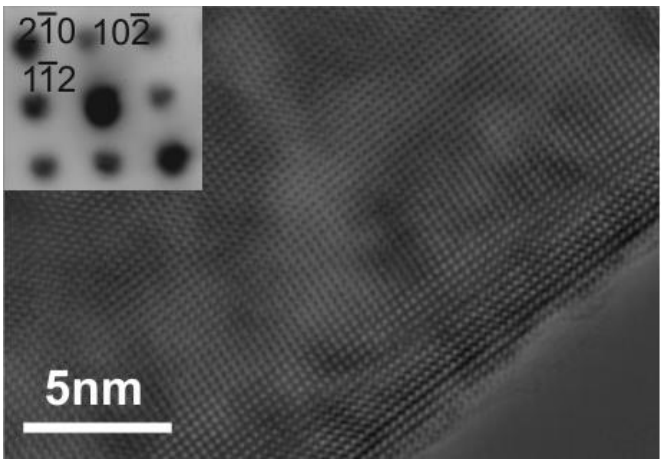

Figure 3. HRTEM image of an Eskolaite crystallite with the corresponding electron diffraction pattern in the inset. Both the image and the EDP are projections along the [2 4 1] zone axis.

Only for P4 as-vitrified product there was no crystalline phase detected in the XRD and SEM analysis. Studying P4 with TEM-HRTEM techniques resulted that there was no indication of any nanostructured products as it is depicted in **Figure 4**. Moreover the EDP had the form of a diffused halo around the transmitted spot which is typical for an amorphous material without any diffraction spots. Thus it is concluded that P4 as-vitrified product retained its amorphous character even in the nanoscale.

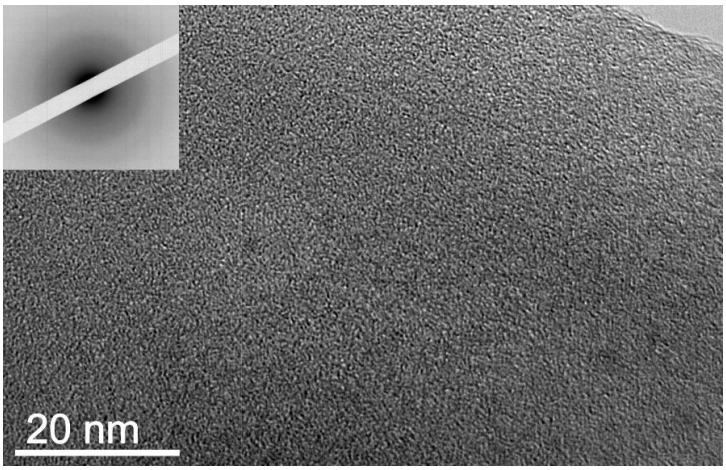

Figure 4. HRTEM image from the homogenous P4 as-vitrified product. The electron diffraction pattern in the inset is a typical of an amorphous material.

Thermal processed products

The vitrified products were conducted to thermal treatment in order to achieve nucleation and crystal growth so as to obtain glass-ceramic products. Devitrification temperatures were determined by DTA analysis and they are listed in **Table 3.** Duration of thermal treatment was set to 30 minutes and the samples were introduced in a preheated oven. Time duration was selected so there would be enough time for the glass formers and fluxes to achieve crystallization. More about the devitrification conditions are reported in a previous work of our group [8].

Table 3: Thermal treatment temperatures

Product	Temperature (°C)
P1	850°C
P2	800°C
P3	920°C
P4	880°C

Devitrification resulted to different separated crystalline phases so as crystallization modes. The composition of separated crystalline phases was depending on the initial batch composition of the parent glass. The Eskolaite crystallites remained unaffected by the thermal treatment. Devitrified products P1-850°C and P2-800°C exhibited surface crystallization and separation of Devitrite ($Na_2Ca_3Si_6O_{16}$). In P3-920°C thermal treatment resulted to the separation of Wollastonite ($CaSiO_3$) and Combeite ($Na_4Ca_4Si_6O_{18}$) in P4-880°C. The separated crystalline phases are indicated on the X-Ray diffractogram in Figure 5 below. The crystalline peaks of each phase are indicated by the respective letters.

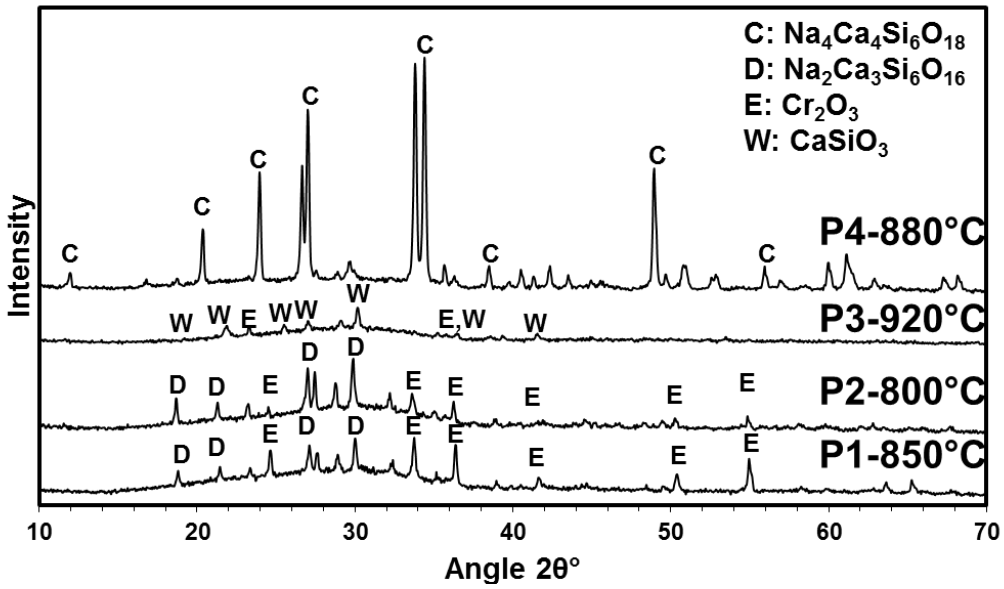

Figure 5. XRD diffraction of all devitrified products.

Transmission electron microscopy (TEM) was utilized to study the structure of these devitrified products at the nanoscale and to verify the different separated crystal phases respectively. In Fig. 6 four different electron diffraction patterns from P1-850°C, P3-920°C and P4-880°C devitrified products are illustrated which correspond to the different separated crystalline phases respectively. The EDP of Fig 6(a) corresponds to a Devitrite crystallite along the [0 0 $\underline{1}$] zone axis from the product P1-850°C. In the case of P3-920°C devitrified product (Figs 6b, 6c) TEM study revealed that except from Wollastonite ($CaSiO_3$), Devitrite ($Na_2Ca_3Si_6O_{16}$) (PDF#23-0671) was also separated during thermal treatment as a secondary phase. This is explained since during the growth of Wollastonite, Ca and Si are being consumed since the remaining matrix is enriched in Na and thus growth of Devitrite is achieved. In the case of Wollastonite, XRD analysis could not define which of the two polymorphs corresponds to the separated crystal phase since the reflections of both correspond to the same 2θ angles and only their intensity varies. Study of the EDP showed that the separated crystalline phase was the triclinic Wollastonite-1A (PDF#73-1110) polymorph. In the case of the devitrified product P4-880°C (Fig 6d) the separated Combeite (PDF#75-1686) crystal phase was verified.

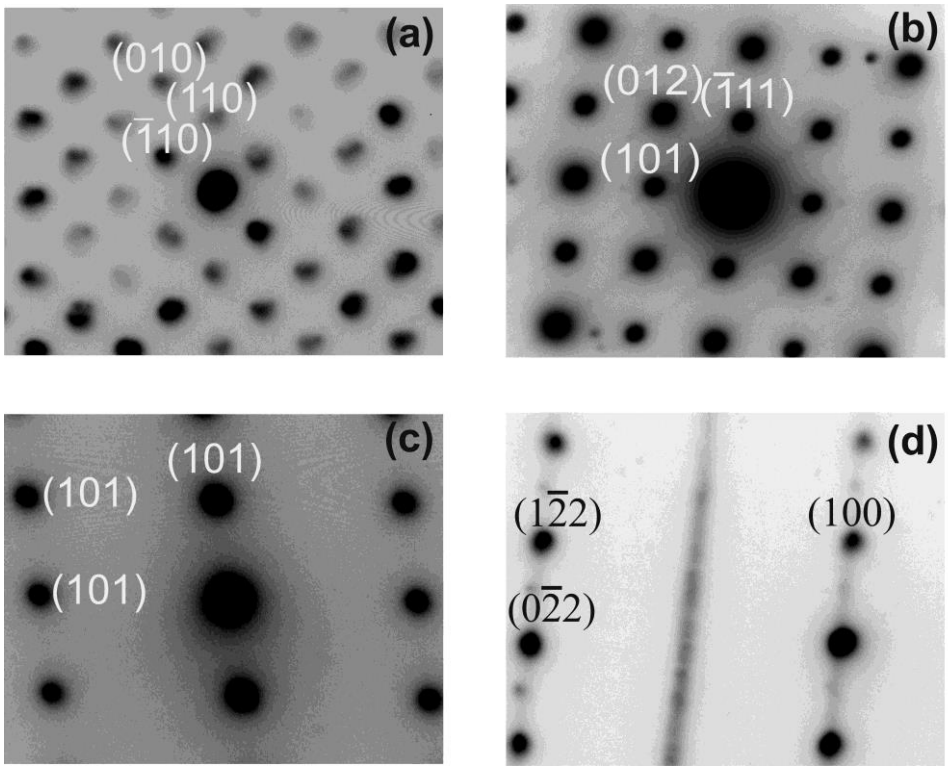

Figure 6. Electron diffraction patterns taken from the separated crystallites of the glass-ceramic products. (a) Devitrite from P1-850°C along the [0 0 1̲] zone axis, (b) Wollastonite from P3-920°C along the [0 1̲ 1̲] zone axis., (c) Devitrite from P3-920°C along the [1 0 1̲] zone axis, (d) Combeite from P4-880°C along the [1̲ 2̲ 1] zone axis.

Figure 7 illustrates a HRTEM image recorded from devitrite in P2-800°C sample, projected along the [01̲0] zone axis. A magnified part is given as inset.

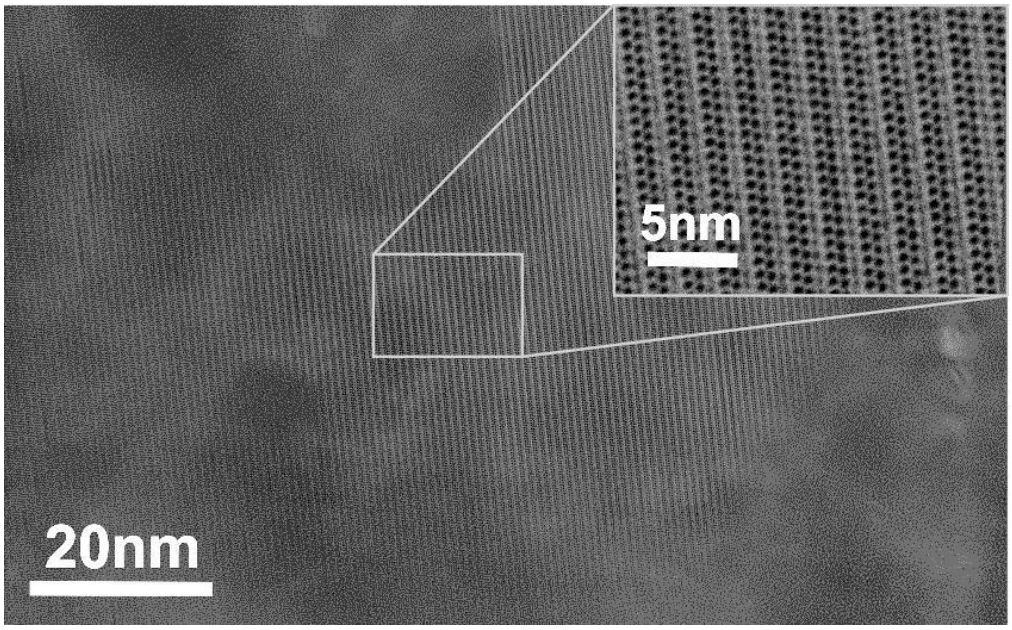

Figure 7. Devitrite HRTEM image from P2-800C devitrified product viewed along the [01̲0] zone axis. In the inset a magnified part of the image.

In P3-920°C crystallization also occurred on the outer surface and Wollastonite ($CaSiO_3$) was separated from the silicate matrix as the main crystalline phase. In Figure 8 a Wollastonite crystal from P3-920°C product is depicted. In the inset. XRD and TEM analysis indicated that Devitrite was also separated as a secondary crystal phase. In the case of Wollastonite, XRD analysis could not define which of the two polymorphs corresponds to the separated crystal phase since the reflections of both correspond to the same 2θ angles and only their intensity varies. Study of the EDP showed that the grown crystal was the triclinic Wollastonite-1A (PDF#73-1110) polymorph.

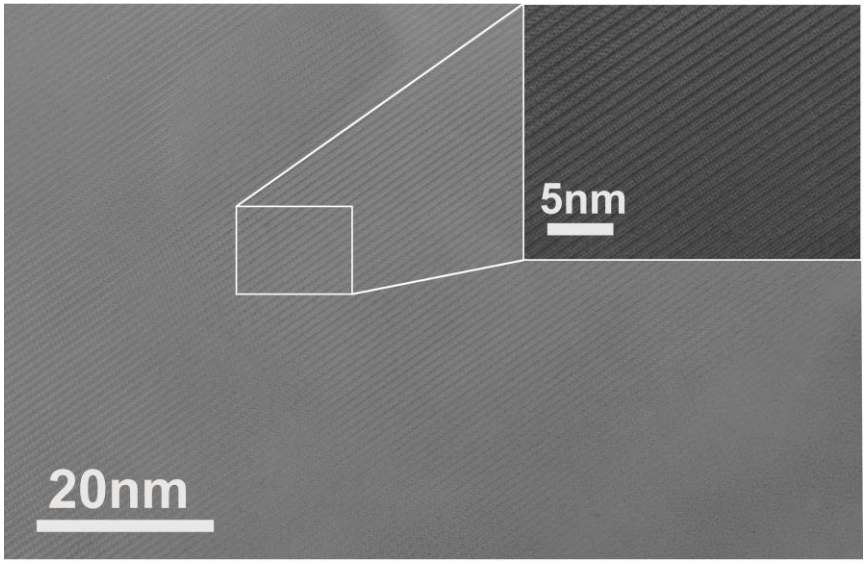

Figure 8. HRTEM image of a Wollastonite crystal from P3-920 ºC devitrified product viewed along the [0$\underline{1}$1] zone axis. A magnified part of the image is given as inset.

P4-880°C devitrified product was the only that exhibited bulk crystallization where crystal growth lead to the separation of Combeite ($Na_4Ca_4Si_6O_{18}$) crystalline phase **(Fig 8-9).**

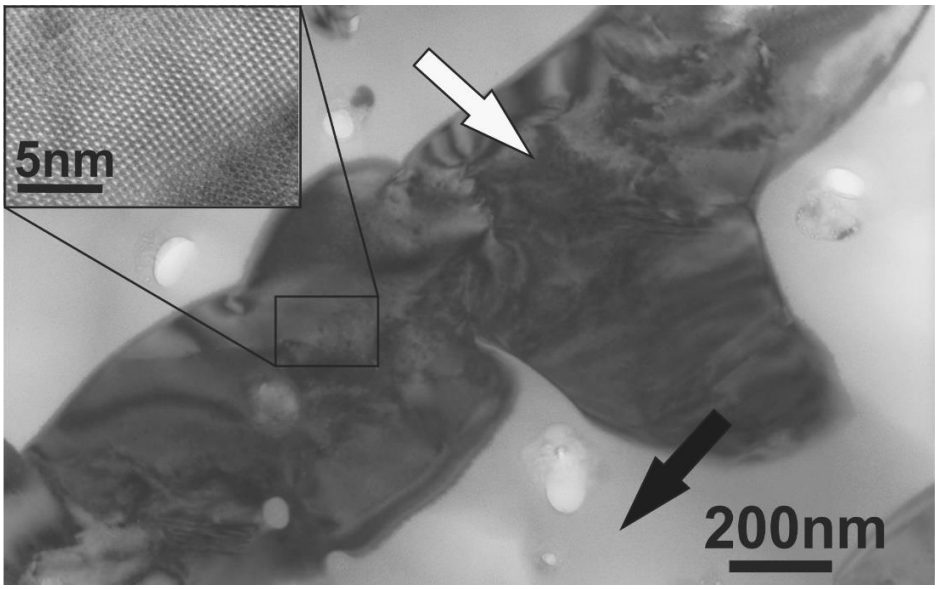

Figure 9: TEM image from a Combeite crystallite in P4-880°C product. The white arrow indicates the crystallite and the black the matrix. The inset shows a HRTEM image of the crystallite recorded from the indicated area. Projection along [$\underline{1}$ $\underline{2}$ 1] zone axis.

Eskolaite crystallites which existed before the thermal treatment remained unaffected. Study of the remaining matrix did not reveal any chromium containing separated crystalline phase also in the thermal treated P4 product. This indicates that Cr remained incorporated in the amorphous silicate matrix.

Chemical analysis with SEM-EDS on the devitrified products showed the distribution of Cr and glass-forming elements inside the samples after thermal processing. In all cases after crystal growth the remaining matrix is enriched in Cr since the new crystal phases do not contain Cr. As a result the proportion of Cr is higher than in the as-casted products. Na proportions became also higher in the remaining matrix in the cases of P1, P2 and P3 devitrified products because the Ca/Na and Si/Na ratios were higher in comparison to their initial glass composition. On the other hand in P4 crystallization of Combeite required more Na and as a result the remaining matrix was enriched in Si and Ca. TEM-EDS analysis was conducted to the as-vitrified and devitrified products to study the distribution of the glass-forming elements and Cr in the samples before and after the thermal treatment but from a nanoscopic point of view. In comparison to the SEM-EDS analysis the distribution of the glass-forming elements and Cr was following the same pattern in the case of the as-casted products. Studying the thermal processed products it was important to define whether during the growth of the new crystalline phases Cr was incorporated inside the crystal structures. The results from the TEM-EDS analysis indicated that there was no Cr incorporated in the grown Devitrite and Wollastonite crystallites in P1, P2 and P3 devitrified products. On the other hand the Combeite crystallites in P4-880 product have some incorporated Cr. This finding agrees with the leaching test results that have been already published by Varitis et. al. [8]. In this case the total leached Cr in the P1, P2 and P3 products was either very low or not detected while in the case of P4 high quantities of leached Cr where detected.

Micro-hardness

The micro-hardness of the vitrified and devitrified products was determined using Knoop geometry and the values are listed in Table 4. Indentation with Vickers geometry was conducted to study the crack propagation in the samples.

Table 4: Micro-hardness values of the as-vitrified and devitrified products

Product	Knoop Micro-hardness (GPa)
P1	5.9±0.2
P1-850°C	7.5±0.3
P2	6.1±0.3
P2-800°C	6.9±0.5
P3	6.3±0.2
P3-920°C	7.3±0.6
P4	6.2±0.1
P4-880°C	6.3±0.3

As it is listed in Table 4 the micro-hardness values of all as-vitrified products was between 5.9- 6.2 GPa. The micro-hardness was increased after thermal treatment and was between 6.3-7.5 GPa.

Comparing the micro-hardness values of the as-vitrified products it has been observed that micro-hardness tends to increase as the CaO content increases and Na_2O decreases. When Na_2O is substituted by CaO even when the network is not depolymerized, the strength of the silicate network increases because Ca^{2+} has greater field strength than Na^+ which strengthens the bonds of the neighboring oxygens [14]. On the other hand decrease of Na content also results to higher micro-hardness [15]. Since the Si/O ratio does have significant variation between the as-vitrified compositions the influence of the ratio and as a result the extent of the silicate network depolymerization is not taken into account.

Comparing the micro-hardness values of the devitrified with the respective values of the initial as-vitrified products heat treatment resulted to an increase in the micro-hardness as it was expected theoretically [11-13]. This increase is attributed to the new crystalline phases that were separated from the silicate matrix which commonly are harder than the amorphous matrix.

Vickers geometry indenter was used to study the crack propagation on the samples surface. In Vickers geometry the applied load was set to 200gf so as to be able to induce isotropic crack propagation .Vickers indentation showed the modes of crack propagation in the as-vitrified products. In the as-vitrified products it was observed that Cr_2O_3 crystallites act as barriers and as a result they are able to contain the crack propagation. The way that the crystallites prevent the crack propagation is illustrated in Figure 10. Studying the products after devitrification it can be concluded that due to their morphology, the separated crystalline phases change the way that a crack propagates. In particular, propagation of cracks follow a mixed pattern and they propagate either intergranular or transgranular to the separated oblong crystallites. Moreover, the crack length decreases significant when the cracks propagate perpendicular to the crystallites. On the other hand, along the oblong crystallites the length size of the cracks is longer since propagation occurs along the interface between the crystallites and the remaining matrix causing interfacial debonding. Comparing the two micrographs in Figures 10 and 11 it is also concluded that the finer crystallites of Wollastonite in P3-920° product allow the radial cracks to propagate longer than the coarser and oblong Devitrite crystallites.

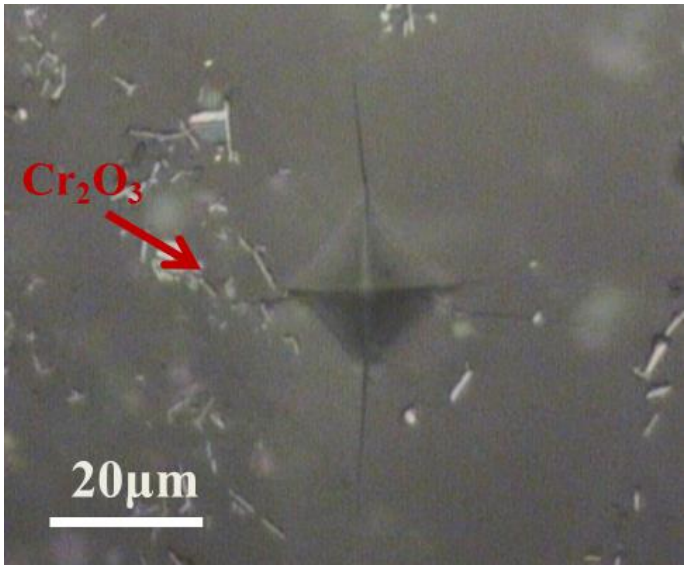

Figure 10: Vickers indentation in the P1-850C devitrified product.

Propagation of the radial cracks produced by the Vickers indentation seems to follow a transgranular pattern since it is affected by the Cr_2O_3 crystallites where the cracks are interrupted. On the other hand cracks propagation is intergranular through the elongated Devitrite crystallites.

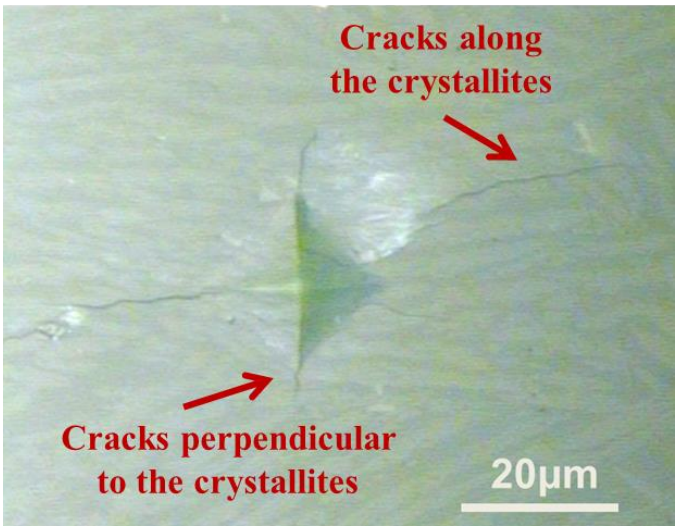

Figure 11: Vickers indentation in the P3-920°C devitrified product.

Conclusions

Electron microscopy and mechanical properties study of vitrified Cr-ash from tannery wastes has been presented in the current work. Vitrification included four different vitrified batch mixtures and their respective glass-ceramic products resulting from the thermal treatment of the parental ones. It has been previously verified that most these products were chemically inert [8]. Structural characterization with electron microscopy techniques (SEM-TEM) indicated that the as-vitrified products were composed of an amorphous matrix and separated Eskolaite crystallites of hexagonal shape, except from one (P4) which was totally amorphous. Moreover through HRTEM observations no nanostructured crystalline phase was detected. Furthermore, thermal treatment of the vitrified products resulted to new separated crystalline phases depending on the initial batch composition. Utilization of TEM verified the structure of separated crystalline phases while HRTEM showed that there were no nanostructured separated crystal phases even after thermal treatment. It was also verified that the grown "Wollastonite" in P3-920°C had triclinic structure of "Wollastonite-1A". Additional it was detected that "Devitrite" was separated as a secondary crystal phase in P3-920°C product. TEM-EDS analysis allowed the study the elemental distribution of Cr inside the amorphous matrix but there was no indication of Cr incorporation inside the grown crystal phases. Microhardness tests concluded that the hardness of the as-vitrified products was in the range of 6.3GPa and it was further increased in the range of 7.5GPa after thermal treatment. Furthermore it was indicated that the dispersed crystallites affect the crack propagation according their morphology and size.

Reference

[1] T. Basegio, A.P. Beck Leao, A.M. Bernardes. C.P. Bergman, Vitrification: An alternative to minimize impact cause by leather industry wastes. J. Haz. Mat. 165, 604-611 (2008)

[2] A.A. Belay, Impacts of Chromium from Tannery Effluent and Evaluation of Alternative Treatment Options. J. Env. Pr. 1, 53-58 (2010)

[3] Avudainayagam S, Megharaj M, Owens G, Kookana RS, Chittleborough D,

Naidu R. Chemistry of chromium in soils with emphasis on tannery waste sites,"

Rev. Environ. Contamin. Toxicol. 178, 53-91 (2003)

[4] Kavouras, P., Komninou, Ph., Chrissafis, K., Kaimakamis, G., Kokkou, S., Paraskevopoulos, K., Karakostas, Th., Microstructural changes of processed vitrified waste products. J. Europ. Ceram. Soc. 23, 1305-1311 (2003)

[5] Colombo, P., Brusatin, G., Bernardo, E., Scarinci, G. Inertization and reuse of waste materials by vitrification and fabrication of glass-based products. Cur. Opin. Sol. Stat. Mater. Sci. 7, 225-239 (2003)

[6] M. D. LaGrega, P.L. Buckingham, J.C. Evans: Hazardous Waste Management, McGraw-Hill International (2nd edition), 2001

[7] P. Kavouras, E. Pantazopoulou, S. Varitis, G. Vourlias, K Chrissafis, G.P. Dimitrakopoulos, M. Mitrakas, A.I. Zouboulis, Th. Karakostas, A. Xenidis. Incineration of tannery sludge under oxic and anoxic conditions: Study of chromium speciation. J. Haz. Mat. 283, 672-679 (2015)

[8] S. Varitis, P. Kavouras, E. Pavlidou, E. Pantazopoulou, G. Vourlias, K. Chrissafis, A.I. Zouboulis, Th. Karakostas, Ph. Komninou "Vitrification of incinerated tannery sludge in silicate matrices for chromium stabilization", Waste Management 59, 237-246 (2017)

[9] H. Khedim, T. Katrina, R. Podor, P.-J. Panteix, C. Rapin, M. Vilasi "Solubility of Cr2O3 and Speciation of Chromium in Soda–Lime–Silicate Melts" J. Am. Ceram. Soc., 93 [5], 1347–1354 (2010)

[10] Huang Deng, Drummond Charles H., Wang Jue, and Blume Russell D., "Incorporation of Chromium(III) and Chromium(VI) Oxides in a Simulated Basaltic, Industrial Waste Glass-Ceramic", J. Am. Ceram. Soc., 87 [11,] 2047–2052 (2004),

[11] Edgar Dutra Zanotto A bright future for glass-ceramics American Ceramic Society Bulletin, Vol. 89, No. 8

[12] Paul "Chemistry of Glasses" 1982 Chapman & Hall

[13] R. D. Rawlings, J. P. Wu, A. R. Boccaccini, Glass-ceramics: Their production from wastes. A Review" Mater. Sci. 41, 733–761 (2006)

[14] W. Vogel "Glass Chemistry" 2nd Edition Springer-Verlag 1994

[15] M. M. Smedskjaer, M. Jensen, Y. Yue "Effect of thermal history and chemical composition on hardness of silicate glasses" J. Non-Cryst Solids 356, 893–897 (2010)